

Self-consistent calculations of interface states and electronic structure of the (110) interfaces of Ge-GaAs and AlAs-GaAs

Warren E. Pickett,* Steven G. Louie,[†] and Marvin L. Cohen

Department of Physics, University of California, Berkeley, California 94720

and Materials and Molecular Research Division, Lawrence Berkeley Laboratory, Berkeley, California 94720

(Received 22 August 1977)

Self-consistent pseudopotential techniques, together with a superlattice geometry, are used to investigate the detailed electronic structure of the (110) interfaces of Ge-GaAs and AlAs-GaAs. For Ge-GaAs six types of interface states are found, all lying below the thermal gap. No interface states are found in AlAs-GaAs. For each interface the total charge density, self-consistent potential, projected band structure, and local density of states are presented. The interface states in Ge-GaAs are discussed in detail. We also present results for the conduction- and valence-band discontinuities at these interfaces, discuss superlattice states in AlAs-GaAs, and suggest possible relaxation at the Ge-GaAs (110) interface.

I. INTRODUCTION

An interface can be defined as the system which results when two differing materials are brought into intimate contact, and the "interfacial region" is that region which differs in its detailed properties from the bulk of either material. It is often convenient, particularly for symmetry considerations, to consider the solid surface as an interface, i.e. the vacuum-solid interface. Many theoretical results for surfaces then are readily generalized to interfaces. For example, Heine's¹ discussion of allowed surface states trivially generalizes to interface states. However, except to allow for such generalizations from "surface" to "interface," in this paper we confine the term interface (IF) to refer only to a solid-solid interface.

Early theoretical considerations of the electronic structure at an IF were confined either to analytic results for highly idealized model systems² or to the qualitative phenomena which may be expected from considerations of symmetry, chemical bonding, or limiting behavior (e.g., nearly free electron or tight binding). While the information gained from these studies is important for pedagogical reasons, it can rarely be applied to a specific system with confidence, and never to give detailed comparison with experiment. That such a detailed interaction of theory and experiment is desirable has been particularly apparent in the use of low-energy-electron diffraction in determining³ surface morphology, which cannot at present be accomplished by either experiment or theory alone.

During the past fifteen years there has been great experimental effort to understand the Schottky barrier⁴ and the heterojunction,^{4,5} as well as more involved systems involving IF's. However, not until recently have there been theoretical attempts to understand in detail the electronic

structure at an IF. The jellium-jellium IF has been studied by a number of researchers⁶ and is rather well understood, although this system enjoys only limited applicability. It is interesting that even in a system of this relative simplicity few analytic results are available. Detailed calculations have now been completed for the covalent semiconductor-jellium IF⁷; these indicate that earlier proposals⁸ for the IF states in the Schottky barrier were incorrect in some important respects.

Attempts to gain detailed information about the semiconductor-semiconductor IF were at first limited to non-self-consistent and crystallographic-IF-independent models which would furnish predictions of the band-edge discontinuities at the IF. These include a simple potential-matching model of Frenley and Kroemer⁹ and a tight-binding-like approach of Harrison.¹⁰ Shay *et al.*¹¹ have revived the idea that, in some sense, a semiconductor-semiconductor IF is equivalent to "canceling" surfaces, which then equates the conduction-band discontinuity across the IF to the difference in electron affinities. Kroemer¹² has emphasized that this model has been treated too often as an exact result in interpreting experimental results. Regardless of the accuracy of these models for the band-edge discontinuities, they provide very little information about other IF properties of interest.

The first self-consistent calculation of an IF electronic structure was by Baraff, Appelbaum, and Hamann (BAH),¹³ who considered an ideal (unfaceted) Ge-GaAs (100) IF. They concentrated on the character of bonds at a polar IF and on the band-edge discontinuities, but were not able to study details such as the spectrum and character of IF states. Moreover, with the geometry used in their study the resulting IF is metallic rather than the experimentally observed semiconductor,

Caruthers and Lin-Chung¹⁴ have since reported non-self-consistent calculations on repeated GaAs-Ga_{1-x}Al_xAs (100) *monolayer* structures. The results indicated that their geometry represents a new compound rather than a series of IF's.

In this paper we present the results of self-consistent calculations of the detailed electronic structure of the ideal (100) IF Ge-GaAs and AlAs-GaAs. Some of the Ge-GaAs results were reported earlier.¹⁵ Perhaps the most important results are that IF states *do occur* in Ge-GaAs (but below the valence-band maximum) but *do not occur* in AlAs-GaAs. For both IF's we give results for the charge density and potential, the projected band structures, the local density of states at various distances from the IF and the character of the bonds across this nonpolar IF, as well as discussing the band-edge discontinuities. For Ge-GaAs we present the complete spectrum of, and discuss the characters of, the six types (bands) of IF states which are found. Since we find both IF's to be semiconducting as is experimentally known to be the case, we expect these results to be representative of abrupt heterojunctions in most respects. Possible relaxation of the Ge-GaAs IF away from the ideal structure is discussed.

Due to the small lattice mismatches $\sim 0.1\%$ in both Ge-GaAs and AlAs-GaAs, which are among the smallest of any known IF's, it is reasonable to ignore effects due to dislocations or faceting, and to study the results due solely to the variation in potential across the IF. Since Al lies just above Ga, and Ge lies between Ga and As, in the periodic table the variation in potential and atomic size across these IF's should be small and systematic. This is of course why the lattice mismatch is small. In somewhat more generality we can consider the Ge-GaAs IF as the prototype of a system in which the ionicity changes from zero to a moderate positive value across the IF, accompanied by and associated with a *change of symmetry* (from diamond to zincblende lattice types). In the AlAs-GaAs IF there is a smaller change in ionicity which arises only from a change in the strength of the (cation) potential; this becomes the prototype for a system with a small ionicity variation across the IF without any change in symmetry.

The atomic positions near a (110) IF in Ge-GaAs are pictured in Fig. 1. We have chosen to study the (110) IF because, unlike the (100) or (111) IF's, each atomic layer contains equal numbers of cations and anions; i.e., it is nonpolar. For nonpolar IF's all bonds remain saturated, at least on the average, and it is expected (and will be verified) that the ideal geometry will give a semiconducting IF as is observed. As noted by BAH,¹³

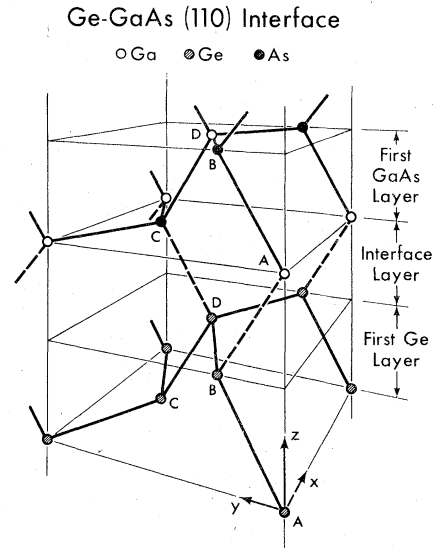


FIG. 1. Atomic positions near the Ge-GaAs (110) interface. Bonds are denoted by heavy solid lines, except bonds across the interface are shown as heavy dashed lines. The chains ABAB and CDBC are the two independent bonding chains perpendicular to the interface, containing the Ge-Ga and Ge-As bonds, respectively. The x , y , and z directions used in setting up the unit cell are shown at bottom.

an unreconstructed geometry at a polar IF must lead to a metallic IF, and the (unknown) atomic rearrangement which finally gives rise to a semiconducting IF is likely to be a crucial feature in polar systems.

The geometry which we will use to study the IF is actually a superlattice, i.e., a periodic array of Ge (or AlAs) and GaAs "slabs." The distance between IF's is chosen large enough that a single isolated IF is well described by the results. This superlattice geometry however provides a bonus, since very recently such superlattices have been synthesized^{16,17} and are found to exhibit numerous interesting properties. Some results relevant to such superlattices will be discussed in Sec. IV.

II. METHOD OF CALCULATION

To study the Ge-GaAs and AlAs-GaAs IF's we have adapted a method of self-consistent pseudopotentials which has been highly successful in surface studies. The method has been described extensively elsewhere¹⁸ so only the basic features will be reviewed here.

An idealized system containing an IF between two semi-infinite solids necessarily lacks periodicity in the direction perpendicular to the IF, taken here as the z direction. The first important feature of the method is that we impose periodicity in the z direction by periodically repeating the IF

TABLE I. Ionic core parameters a_i and empirical starting potential parameters b_i for Al, Ga, Ge, and As. The potentials are normalized to a volume of 152.9 a.u.³. The forms of the potentials are given by (1) and (2). With q given in atomic units, the potential is in rydbergs. (The Ga potential is valid only for $q \leq 3$ a.u.)

Potential parameters	Al	Ga	Ge	As
a_1	-0.569 18	-0.338 45	-0.955 46	-0.704 51
a_2	1.046 80	1.330 50	0.803 23	1.044 80
a_3	-0.133 89	0.456 60	-0.312 05	0.166 24
a_4	-0.029 44	0.007 05	-0.018 52	-0.015 12
b_1	0.448 9	10.217 9	2.417 2	1.132 1
b_2	1.880 0	2.384 6	2.414 7	2.653 3
b_3	0.650 0	0.559 8	0.583 7	0.682 5
b_4	-0.300	-6.475 4	-3.404 4	-1.276 9

geometry. By retaining a periodic system in this way the usual “ k -space methods” of the pseudopotential technique can be applied. In addition we require the IF’s to be far enough apart that the “interfacial regions” do not overlap. This satisfies the primary desire that each IF is independent of all other, since we wish to study the properties of a single isolated IF. An equivalent requirement is that the local material properties midway between IF’s should be representative of the bulk solid.

Specifically we have chosen a unit cell having 18 layers (9 of each material) in the z direction. As each (110) plane contains 2 atoms/(unit cell), the unit cell contains 36 atoms and *two* IF’s. We demonstrate below that the IF’s so described are independent to high accuracy. We also note that, since the unit cell is so long in the z direction, the Brillouin zone is effectively two dimensional (in the x - y plane), as would hold exactly for a single isolated IF.

The inputs to the calculation are the atomic positions within the unit cell and the ion core pseudopotentials used to describe the ions. The ionic positions, shown in Fig. 1, are those appropriate to a diamond lattice of cubic lattice constant $a_0 = 10.696$ a.u., essentially equal to that of bulk Ge, GaAs, or AlAs. The ion-core pseudopotentials V_{ion} are parametrized in the form

$$V_{\text{ion}}(q) = (a_1/q^2)[\cos(a_2q) + a_3]e^{a_4q^4}, \quad (1)$$

where the parameters a_i are fit to a Heine-Abarenkov core potential, and in some cases are slightly adjusted further to give a good bulk band structure. Once these parameters are fit, however, there is *no additional adjustment* to describe IF features. The parameters a_i for Ge, Ga, As, and Al which were used in the calculation are listed in Table I, and the ionic potentials in real space are pictured

in Fig. 2.

For large r the ion-core potential must have the asymptotic form $V_{\text{ion}}(r) \rightarrow -ze^2/r$ for ionic charge z . This leads to the constraint $a_1(1+a_3) = -4\pi z e^2/\Omega_a$, where Ω_a denotes the atomic volume. For surface calculations this constraint has sometimes been relaxed. However, since for the IF we will be particularly interested in obtaining an

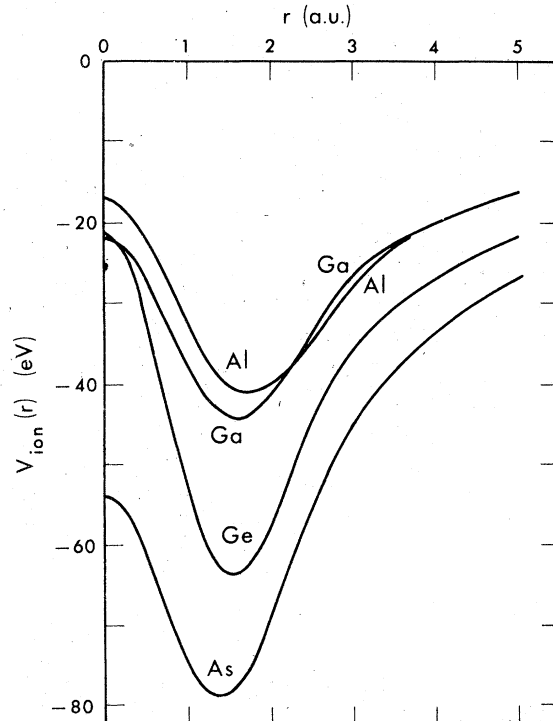


FIG. 2. Ionic pseudopotentials of Al, Ga, Ge, and As, plotted in real space, showing their relative strengths. The potential for $r \leq 1$ a.u. is somewhat arbitrary.

accurate evaluation of the electrostatic dipole from the electronic charge density and ionic charges, this constraint has *not* been relaxed for these calculations.

The ion core potentials must be screened self-consistently by the valence electron potential. A basis set of approximately 430 plane waves has been used to obtain accurate energies and wave functions, and an additional ~ 750 plane waves were incorporated into the calculation via a second-order perturbation scheme, the screening potential is then derived from the charge density formed by summing over occupied states.

To begin the self-consistency procedure we have used an empirical (screened) potential of the form

$$V_{\text{emp}}(q) = b_1(q^2 - b_2) / \{\exp[b_3(q^2 - b_4)] + 1\}. \quad (2)$$

The parameters b_i are fitted to reproduce the bulk band structure and are also listed in Table II. Since small q values are not present in the fitting procedure the empirical potential is not expected to be accurate in this region; however, this potential is only used to initiate iteration and will not affect the self-consistent results.

Given the starting potential, the wave functions are calculated with a plane-wave basis, ultimately leading to the total charge density $\rho(\vec{r})$ in terms of its Fourier components $\rho(\vec{G})$. From the charge density we derive a Hartree screening potential V_H and an exchange-correlation potential V_x (in the local-density approximation) as has been described previously.¹⁸

The (110) IF's of both Ge-GaAs and AlAs-GaAs are found experimentally to be semiconducting. As long as the system remains semiconducting during the iteration procedure it is permissible (and time saving) to use well-characterized special points schemes.¹⁹ These schemes allow the use of only a small number of special points in the Brillouin zone to yield an accurate charge density. We have used the set of four special points

$(\frac{1}{8}, \frac{1}{8})$, $(\frac{1}{8}, \frac{3}{8})$, $(\frac{3}{8}, \frac{1}{8})$, $(\frac{3}{8}, \frac{3}{8})$ in the rectangular two-dimensional zone (reduced units for wave vectors are used here and below) for the iteration process.

In spite of the previously noted¹⁸ highly nonlinear nature of the self-consistency process, careful mixing of input and output potentials to produce a new input potential will yield convergence in 5–10 iterations. In the case of Ge-GaAs, iteration was continued until each Fourier component of the potential was self-consistent to within 4×10^{-4} Ry. Such an extreme requirement of self-consistency is unnecessary, and in the AlAs-GaAs calculation iteration was terminated when Fourier components of the input and output potentials agreed to within 2×10^{-3} Ry. The eigenvalues are self-consistent to roughly the same order and in fact converge more rapidly than the small- G components of the potential, which are very sensitive to small charge transfers across the IF.

The procedure for obtaining the local and total density of states is well known. We have used the wave functions and eigenvalues at 13 k points in the irreducible zone (a total of 936 independent valence eigenvalues) with a histogram channel width of 0.1 eV to generate the density of states plots shown below.

An idea of the importance of self-consistency can be obtained from Fig. 3, where the total potential, averaged parallel to the IF, is shown for the empirical potential and the resulting self-consistent potential for both IF's. In general, there are two primary differences between the empirical and self-consistent potentials. Firstly, the relative positions of the energy about which the potential oscillates on each side of the IF (the average bulk potential \bar{V}) is changed considerably during iteration. For the Ge-GaAs IF, the empirical value of $(\bar{V}_{\text{Ge}} - \bar{V}_{\text{GaAs}})_{\text{emp}} = 0.75$ eV is reduced to a final value of $\bar{V}_{\text{Ge}} - \bar{V}_{\text{GaAs}} = 0.25$ eV. In AlAs-GaAs the effect is more dramatic, with the initial value of 1.70 eV being changed to the final value of $\bar{V}_{\text{AlAs}} - \bar{V}_{\text{GaAs}} = -0.05$ eV. Secondly, the change in empirical po-

TABLE II. Schematic comparison of the localized states of the GaAs (110) surface (Ref. 18) and the Ge-GaAs (110) interface (this work). The energy of each localized state ("feature") is given on the scale used for the interface. Qualitative interconnections are denoted by arrows.

GaAs (110) surface		Ge-GaAs (110) interface	
Feature	Energy (eV)	Energy (eV)	Feature
As <i>s</i> like	-9.25	-11.5	As <i>s</i> like (S_1)
Ga <i>s</i> like	-6.00	-6.0	Ga <i>s</i> like (S_2)
As back bond	-2.25	-4.0	Ge-As bond (B_1)
As parallel bond	-0.75	-2.25	"Ga-As" parallel bond (P_1)
As dangling bond	-0.50	-1.0	"Ge-Ge" parallel bond (P_2)
Ga dangling bond	0.75	-1.0	Ge-Ga bond (B_2)

tential across the IF is localized almost entirely in the region between the two atomic planes bordering the IF, whereas the self-consistent potential changes rather slowly over ~ 4 atomic planes (in Ge-GaAs). This is primarily because the empirical potential represents individual screened ions which (i) have a short range, and (ii) are identical at the IF and far from the IF. Together these properties result in an abrupt change from one bulk material to another. The self-consistent screening of ionic pseudopotentials allows the total valence electron density to "see" each ion and readjust accordingly, resulting in a more gradual transition at the IF.

Each of these effects of self-consistency may be important. The particular form of the potential at the IF, and whether it is a gradual or abrupt change, will obviously greatly affect the possible formation of IF states, as well as influencing the charge density (and hence bonding properties) across the IF. For example, the Ge-GaAs IF states discussed in Sec. III appeared as well-localized IF states only after $\sim 3-4$ iterations. The relative positions of the average bulk potentials, which then determine the relative positions of the two bulk band structures, determine the valence- and conduction-band discontinuities across the IF, which are quantities which have received considerable experimental attention due to their importance in device applications. The relative positions of the bulk band structures also determine allowed regions for true IF states, which may exist¹ only in coinciding gaps in the two projected band structures.

Since the empirical potential is used only to initiate the self-consistency procedure one might question the relevance of any comparison of initial and final potential. The significance comes from the fact that, within a pseudopotential approach, the empirical potential represents a reasonable "best guess" if self-consistency is not to be attempted. While the form we have chosen is reasonable, it is not unique, being only one of many possible, but similar, forms. Any given form must interpolate between a few values $V_{\text{emp}}(G)$ (known for small bulk reciprocal lattice vectors G) and extrapolate to zero for $q \rightarrow \infty$ and to $\sim -\frac{2}{3}E_F$ (Fermi energy) for $q \rightarrow 0$. Any reasonable empirical potential will however lead to an abrupt change in the potential across the IF, due to its short range.

To facilitate the identification and classification of IF states we have carried out self-consistent calculations of the bulk band structures of Ge, GaAs, and AlAs using the potentials of Table I and Fig. 2. For each material the (110) projected band structure (PBS) was then derived, and, for each IF, the PBS's was positioned relative to each

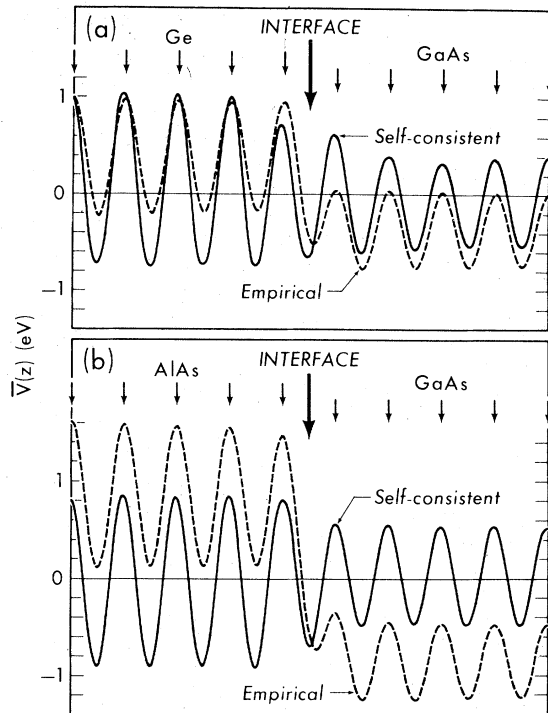


FIG. 3. Empirical and self-consistent potentials, averaged parallel to the interface, for the (110) interfaces of (a) Ge-GaAs and (b) AlAs-GaAs. The large arrow denotes the geometric interface, while the smaller arrows show the positions of atomic planes. One-half of the unit cell in the z direction is pictured.

other by aligning the average bulk potential (taken as zero in bulk calculations) with that resulting from the IF calculations, pictured in Fig. 3. Allowed true IF states can exist only in the surviving gaps of both PBS's. The results are discussed separately for the two IF's in Sec. III.

III. RESULTS

A. Ge-GaAs (110) interface

The total self-consistent valence electron charge density for the Ge-GaAs (110) IF is shown in Fig. 4. The charge density is pictured for two planes perpendicular to the IF, with one containing the Ge-Ba bond and the other containing the Ge-As bond across the IF. The charge density on each side more than two atomic layers from the interface is representative of the respective bulk charge density.²⁰ This indicates that the IF shown is effectively "isolated" from the other IF's. In addition, it demonstrates that the basis set we have used (~ 1000 plane waves) is sufficiently complete to give a good representation of the charge density.

It is apparent that the Ge-Ga and Ge-As bonds are significantly different from either the Ge-Ge

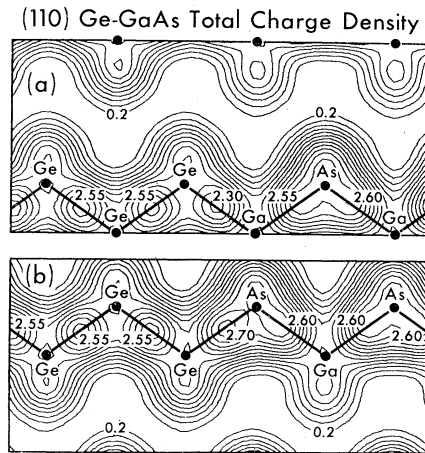


FIG. 4. Contour plot of the total self-consistent valence charge density of Ge-GaAs, pictured in the planes perpendicular to the interface containing the *ABAB* (a) and *CDCD* (b) chains of Fig. 1. Only one-third of the unit cell, centered at an interface, is pictured. The average charge density is normalized to unity; successive contours are separated by 0.2 units. Note that the Ge-Ga and Ge-As bonds across the interface are unlike both the Ge-Ge or Ga-As bonds. The maximum charge density in the bonding regions are quoted to the nearest 0.05 units.

or Ga-As bonds. The charge density maxima for the two types of bulk bonds are approximately equal (~ 2.55 – 2.60 when the average charge density is normalized to unity). The maximum of the Ge-Ga (resp. Ge-As) bond is $\sim 8\%$ – 10% less than (greater than) that of the bulk bonds. This behavior is roughly what would be expected from the following simple chemical consideration. Since (Ga, Ge, As) contribute (3, 4, 5) electrons to their four tetrahedral bonds, they contribute (0.75, 1.00, 1.25) electrons/bond. This leads to an initial estimate of 1.75 and 2.25 electrons for the Ge-Ga and Ge-As bonds.

To check the applicability of this naive argument to the bond charges at a nonpolar IF, we have calculated the total charge in various regions within the unit cell which contain a single bond. Whereas each bond which does not cross the IF is found to contain two electrons (to an accuracy of 0.2%), we find that the Ge-Ga and Ge-As bonds across the IF contain 1.89 and 2.11 electrons, respectively. Thus the bond charges at this Ge-GaAs IF are *significantly more uniform* than simple (and non-self-consistent) chemical considerations would indicate. We emphasize that even the Ge-Ge and Ga-As bonds parallel to and bordering the IF contain 2 electrons to high accuracy. Implications of this charge transfer between bonds across the IF will be discussed in Sec. IV.

The most intriguing result of this study is the

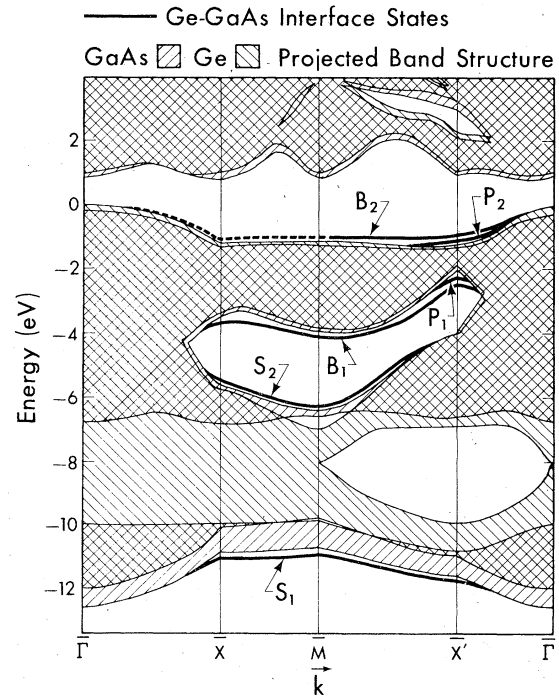


FIG. 5. Interface states of (110) Ge-GaAs relative to the projected band structures of bulk Ge and GaAs from self-consistent calculations. The dispersion of the interface states is denoted by heavy solid lines; heavy dashed lines indicate interface states which have a long decay length into the bulk. Symmetry points (in reduced units) are $\bar{\Gamma} = (0, 0)$, $\bar{X} = (\frac{1}{2}, 0)$, $\bar{M} = (\frac{1}{2}, \frac{1}{2})$, $\bar{X}' = (0, \frac{1}{2})$. The interface states S_1 , S_2 , B_1 , B_2 , P_1 , P_2 , as well as the "stomach" gap (-2 to -6 eV) and the "lower" gap (-7 to -10 eV) are described in the text.

discovery of IF states in Ge-GaAs. The spectrum of true IF states is shown in Fig. 5, together with the (110) PBS's of Ge and GaAs. IF states are allowed only in the gaps in Fig. 5, i.e., in the fundamental gap (-1 to 2 eV), in the "stomach" gap (-2 to -6 eV), in the "lower" gap (-7 to -10 eV), and below the valence bands (< -11 eV). Small gaps exist in the lower conduction bands as well, but appear in these calculations to be of no consequence. Six types (or partial bands) of IF states are found to exist in the valence band region, primarily near the edges ($\bar{X} \rightarrow \bar{M} \rightarrow \bar{X}'$) of the two-dimensional Brillouin zone. The charge densities of these states are presented in Figs. 6 and 7 in the plane(s) in which the state is concentrated. It is convenient to discuss the IF states in pairs.

The states labeled S_1 and S_2 are *s*-like IF states derived from the As and Ga atoms, respectively, at the IF. S_1 lies just below the As-derived bulk valence bands and, like the other IF states, merges into the PBS away from the zone edges. The charge density is primarily spherical, with a

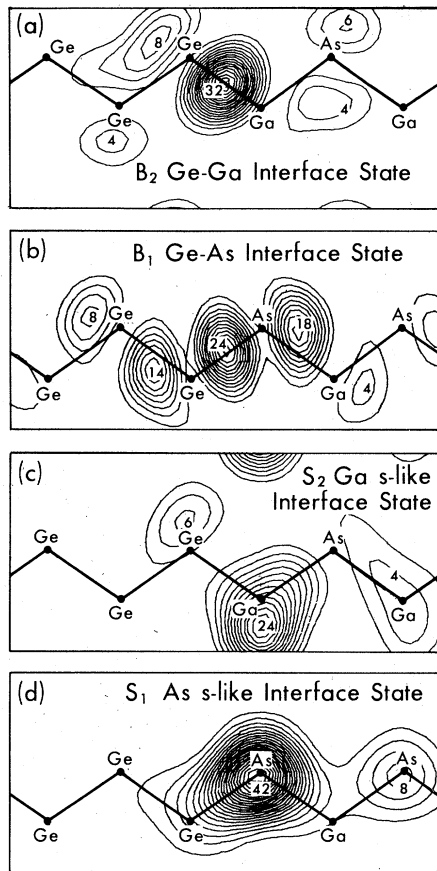


FIG. 6. Contour plots, perpendicular to the interface, of the charge densities of the interface states S_1 , S_2 , B_1 , B_2 . Each averaged charge density is normalized to unity; successive contours are separated by 2.0 units. Straight lines denote bond directions. The interface states derived from the Ga (respectively, As) are plotted in the plane of the $ABAB$ (respectively, $CD CD$) chain in Fig. 1. In each case the charge density in the plane which is not shown is $< 5\%$ of that in the plane shown.

small bulge toward each of the three neighboring Ga atoms [only one of which is shown in Fig. 6(d)] and a larger bulge toward the neighboring Ge atoms, and small contributions ($\sim 5\%$) from As atoms in the second and third layers away from the IF. The S_2 state lies near the bottom of the stomach gap and, although roughly spherical except for bulges toward neighboring As atoms [as shown in Fig. 6(c)], it is not centered on the Ga atom. The center is shifted $\sim 0.7 \text{ \AA}$ parallel to the IF and toward the midpoint of the two neighboring As atoms, due to the weaker Ge potential relative to that of As .

The states B_1 and B_2 are, respectively, Ge - As and Ge - Ga p -like bonding states directed across the IF, as shown in the charge-density plots of

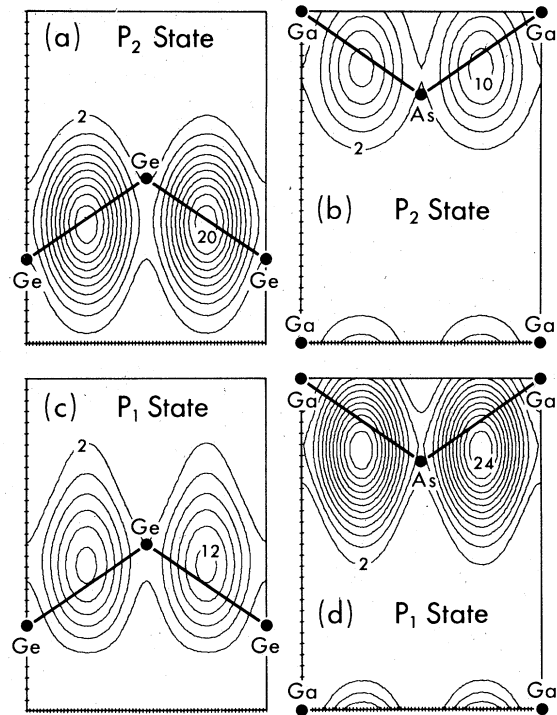


FIG. 7. Contour plots, in planes parallel to and adjacent to the interface, of the parallel bonding interface states P_2 [(a) and (b)] and P_1 [(c) and (d)]. The average charge density of each state is normalized to unity; successive contours are separated by 2.0 units. Less than 10% of the charge of each state lies in the other atomic layers combined. The states are described more fully in the text.

Figs. 6(a) and 6(b). B_1 runs along the top of the stomach gap; B_2 lies at the bottom of the fundamental gap and exists over $\sim \frac{2}{3}$ of the Brillouin zone. The charge density of the B_1 state is strongly concentrated between the Ge and Ga atoms, whereas B_2 , with its central maximum between Ge and As and its subsidiary maxima "behind" the atoms, resembles the classic picture of bonding p orbitals.

A simple consideration of the potential provides some understanding of these IF states. The ionic potential in the bonding region between the Ge and As atoms at the IF is stronger than that in bulk Ge and $GaAs$. The As -related states S_1 and B_1 respond to this negative perturbation and drop in energy below their bulk counterparts. Conversely, the Ga -related states S_2 and B_2 are pushed higher in energy by the relatively weaker ionic potential in the Ge - Ga bonding region.

The states denoted P_1 and P_2 exist only near the symmetry point \bar{X}' and are derived from Ge - Ge and Ga - As bonds adjacent to and parallel to the IF. The charge densities of these states are pic-

tured in Fig. 7. The charge density of each state is shown in the atomic planes *parallel* to the IF, since very little of the charge lies in the planes across the IF depicted in Fig. 6. Both P_1 and P_2 have contributions from the Ge-Ge and Ga-As bonds parallel to the IF, the primary distinction being the relative contribution from each: P_1 is $\sim \frac{2}{3}$ Ga-As, whereas P_2 is $\sim \frac{2}{3}$ Ge-Ge. A further difference is that the charge density peaks of P_2 lie nearly on the line joining nearest neighbors whereas those P_1 are significantly shifted from that line.

The formation of these states is not easily understood in terms of ionic potentials as was the case for S_1 , S_2 , B_1 , and B_2 . However, we note that the shift of the charge-density peaks in P_1 on the Ge atomic plane is toward the Ge with an As, rather than Ga, nearest neighbor across the IF. In the GaAs atomic plane the shift is toward the Ge-As bond rather than the Ge-Ga bond. It may also be of some relevance that the state (P_1) with most charge density in the more ionic material (GaAs) lies lowest in energy.

The local density of states (LDOS) of this IF is shown in Fig. 8. The regions of integration; i.e., IF layer, first Ge layer, first GaAs layer (to be denoted below as [IF], $[\text{Ge}]_1$, $[\text{GaAs}]_1$), etc. are rectangular regions bounded by the atomic layers and are pictured in Fig. 1. Also shown in Fig. 8 is the "excess" LDOS, defined as the amount by which the LDOS exceeds *both* bulk state densities, if positive. This excess LDOS denotes states which must necessarily be localized at the layer under consideration.

The LDOS in $[\text{Ge}]_2$ [Fig. 8(a)] is similar to that of bulk Ge except at the energy ~ -8 eV, where long-range order in the bulk causes the state density to vanish at one point. The effect of the IF on this layer is only to destroy some long-range order, giving changes reminiscent of amorphous semiconductor calculations. In $[\text{Ge}]_1$ these effects increase and in addition an appreciable excess LDOS appears at -1 to 0 eV, from the B_2 and P_2 states, and in the region -10 to -7 eV. This latter is due to IF resonances (R_1) surrounding the lower gap in Fig. 5. These resonances correspond to Ge bulk states in the region of the GaAs "anti-symmetric gap." Since it is impossible for propagating states at this energy to exist in GaAs, the Ge states are reflected at the IF. The R_1 resonances can be interpreted as constructively interfering incident and reflected waves. They are similar to the "metal-induced gap states" in the metal-semiconductor interface.⁷

At the IF layer [IF] the LDOS is distorted in the region -12 to -8 eV, the peak at -12 to -11 eV arising from As s states and the remainder being

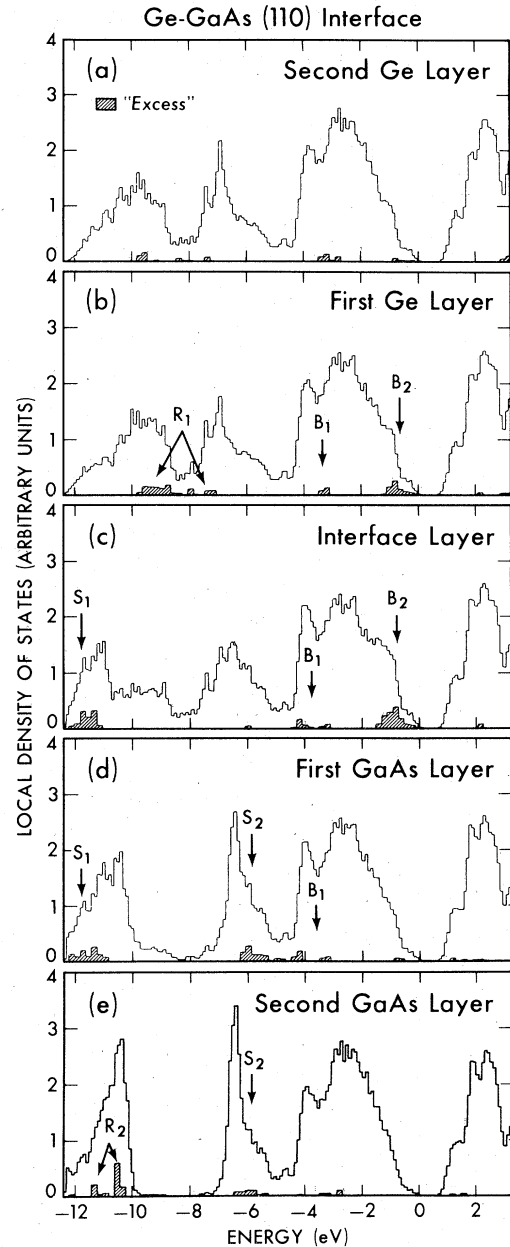


FIG. 8. Local density of states for five layers surrounding the Ge-GaAs (110) interface. The "excess" denotes the density of states localized at the layer as described in the text. The designations "Interface Layer," "first Ge layer," etc. are as pictured in Fig. 1. The positions of the interface states (S_1 , S_2 , B_1 , B_2) and resonances (R_1 , R_2) from which localized states arise are pictured. The local density of states in layers farther from the interface is essentially bulklike.

due to Ge. In the excess LDOS the S_1 state and B_2 (and possibly P_2) states produce features which may be measurable in very careful photoemission experiments; the B_1 and P_1 states are hardly no-

ticeable. In $[\text{GaAs}]_1$ the As state S_1 remains, together with most of the charge density of the Ga state S_2 . The LDOS is noticeably GaAs like, with the antisymmetric gap rather well formed. In $[\text{GaAs}]_2$ the LDOS is distinctly that of GaAs. The band-edge tails in the antisymmetric gap are due to the lack of true long-range order. The excess LDOS contributions at -11 to -10 eV arise from GaAs resonances R_2 near the edge of the Brillouin zone.

Integrating the LDOS over the valence band gives the charge in each layer. We have found that each layer throughout the unit cell contains 8 electrons to an accuracy of $\sim 0.3\%$. The calculated electrostatic dipole, defined by

$$d = 4\pi e^2 \int (z - \bar{z}) \bar{\rho}(z) dz, \quad (3)$$

where \bar{z} is the position of the IF and $\bar{\rho}(z)$ is the charge density averaged parallel to the IF, is $d \approx 0.10$ eV and tending to raise Ge relative to GaAs.

The difference in energy gaps for this IF is $\Delta E_g = E_g^{\text{GaAs}} - E_g^{\text{Ge}} = 0.75$ eV. The manner in which ΔE_g is distributed between the valence and conduction bands is of crucial importance in understanding the electrical and optical properties of Ge-GaAs heterojunctions. From Fig. 3(a) the difference in average potential \bar{V} is $\bar{V}^{\text{Ge}} - \bar{V}^{\text{GaAs}} = 0.25$ eV. Referencing the valence-band maximum to the average potential in the bulk band structures and raising Ge by 0.25 eV gives a valence-band discontinuity $\Delta E_v = E_v^{\text{Ge}} - E_v^{\text{GaAs}} = 0.35$ eV, which leaves a similar discontinuity $\Delta E_c = E_c^{\text{GaAs}} - E_c^{\text{Ge}} = 0.40$ eV. In arriving at ΔE_c we use ΔE_v and the experimental gap values, since the conduction-band minimum is quite sensitive to the ionic potential, causing the gaps to be ~ 0.2 eV in error. We estimate our overall error to be ~ 0.1 – 0.2 eV.

A number of capacitance-voltage (C-V) and current-voltage (I-V) measurements have been used to extract values of ΔE_c in the Ge-GaAs heterojunctions. If all recent measurements are given weight a value of 0.2 ± 0.15 eV is obtained. A further discussion of the band-edge discontinuities and their comparison with experiment is presented in the Sec. IV, where the AlAs-GaAs results can be included.

B. AlAs-GaAs (110) interface

In Fig. 9 the total self-consistent charge density for the AlAs-GaAs (110) IF is presented, in the same two planes perpendicular to the IF as in Ge-GaAs (Fig. 4). Again the charge density away from the IF is representative of the respective bulk charge density.²¹ Unlike the Ge-GaAs IF, however, there is virtually no disruption of the charge

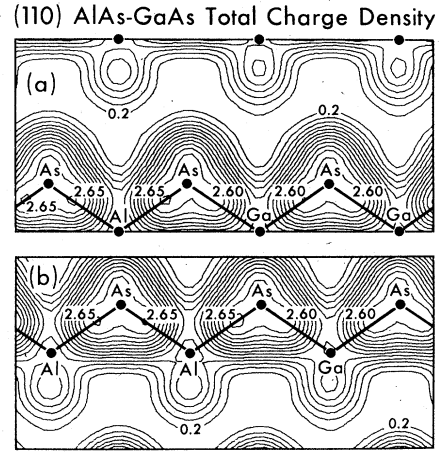


FIG. 9. Contour plot of the total self-consistent valence charge density of AlAs-GaAs, using the same geometry and conventions as in Fig. 4. Note that the Al-As and Ga-As bonds across the interface are essentially the same as those in the respective bulk material.

density at the IF. In fact, both the Ga-As and Al-As bonds across the IF are like the bonds in the bulk. The bonding charge parallel to the IF is also not significantly altered from the respective bulk counterparts. The variation across the IF, in this case a small change in ionicity, is accommodated in a very localized manner across the As atom at the IF. The charge transfer from the Ga-As bond to the Al-As bond at the IF (or elsewhere) is negligible (≈ 0.002 electron).

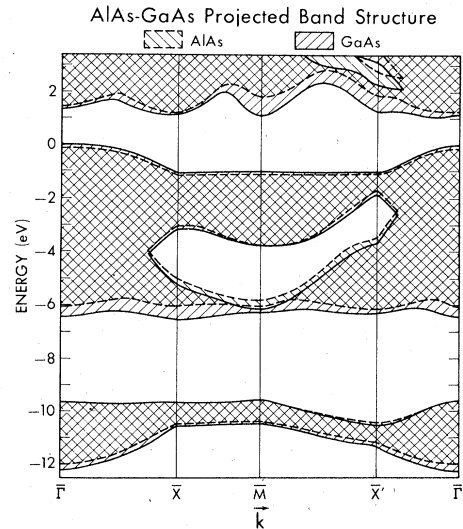


FIG. 10. (110) projected band structures of bulk AlAs and GaAs from self-consistent calculations. No interface states are found to exist in either the fundamental gap (0 to 2 eV), the "stomach" gap (-6 to -2 eV) or the antisymmetric gap (-10 to -7 eV), or below the valence bands (< 11 eV). Symmetry points are as in Fig. 5.

No IF states are found in the AlAs-GaAs (110) IF. The PBSs of AlAs and GaAs are shown in Fig. 10. The differences in the PBSs in the valence band region (negative energies) can all be accounted for by the increased ionicity of AlAs relative to GaAs. The As *s*-derived bands (-10 to -12 eV) are similar in these materials. The largest difference occurs in the lower bonding states (-4 to -6 eV) which have a large contribution from the cation. Due to the deeper potential in Ga relative to As (see Fig. 2), these states lie ~ 0.5 eV lower in GaAs. The differences in the conduction-band region are dependent on the details of the potentials.

In Fig. 11 we present the LDOS and "excess" for three layers near the IF. As would be expected from the PBS's of Fig. 10 there is very little change in the LDOS across the IF except for slight variations in the antisymmetric and fundamental gaps. The excess LDOS, which is determined by localized states (true IF states and resonances),

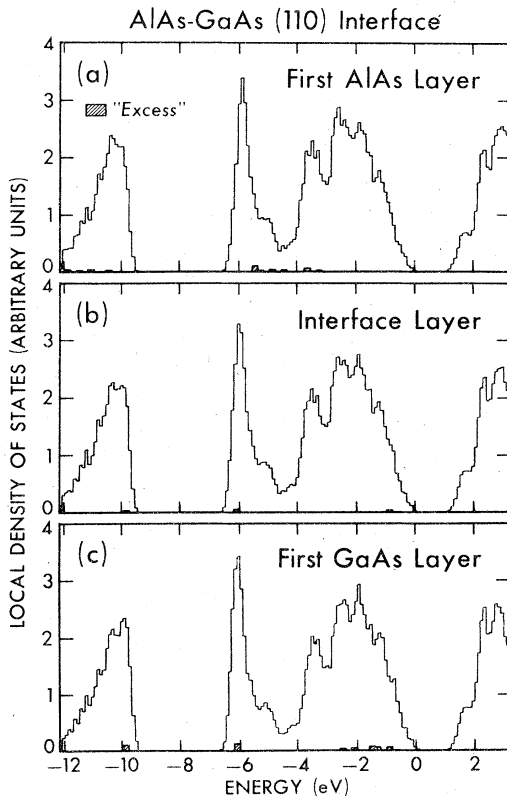


FIG. 11. Local density of states for three layers surrounding the AlAs-GaAs (110) interface. The notation is as in Fig. 8. The localized states as described by the "excess" local density of states is extremely small for this interface. The density of states at layers farther from the interface than those shown is essentially bulklike.

is completely negligible at the IF layer and the contributions from resonances in $[\text{AlAs}]_1$ and $[\text{GaAs}]_1$ are very small. The excess vanishes for layers further from the IF. Integrating the LDOS (as described previously for Ge-GaAs) indicates that each layer in the unit cell contains 8 electrons. The electrostatic dipole for this IF is entirely negligible.

The difference in experimental thermal gap values²² for these materials is $\Delta E_g = E_g^{\text{AlAs}} - E_g^{\text{GaAs}} = 2.1 - 1.45 = 0.65$ eV. However, the AlAs gap is indirect while that of GaAs is direct. Since we must compare band-edge discontinuities with experimental values for $\text{Al}_x\text{Ga}_{1-x}\text{As-GaAs}$ ($x \approx 0.2$) in which the gap is direct, it is appropriate to use the *direct* gaps at Γ and assume linear extrapolation of this gap for $x \rightarrow 1$. Then we obtain²² $\Delta E_g^{\text{dir}} = 2.9 - 1.45 = 1.45$ eV. The most recent experiments^{23,24} give $\Delta E_v = (0.15 \pm 0.03)E_g^{\text{dir}}$. We obtain $\Delta E_v = 0.25$ eV $= 0.17\Delta E_g^{\text{dir}}$, in excellent agreement with the experimental results. These band-edge discontinuities are discussed further in Sec. IV.

IV. DISCUSSION

In Sec. III we have presented and discussed separately the results of microscopic electronic structure calculations of the ideal Ge-GaAs and AlAs-GaAs (110) IF's. To facilitate a more general understanding of IF structure we present in this section a comparison of certain features of these two interfaces, with each other, with experiments, and with the corresponding ideal surfaces. The peculiar bonds across the Ge-GaAs IF suggest atomic relaxation at this IF, of which two possibilities are suggested. Superlattice aspects which may be of experimental interest are also presented and discussed.

A. Band-edge discontinuities and interface states

Experimentally the two most accessible microscopic properties of an IF are the discontinuities of the valence and conduction bands across the IF and the existence of IF states. According to most models used to interpret the experimental *I-V*, *C-V*, and optical data, only IF states in the thermal gap (between valence-band maximum and conduction-band minimum) will substantially affect these data. In both AlAs-GaAs and Ge-GaAs the density of IF states in the thermal gap is found^{4,5} to be very (usually undetectably) small, and can be accounted for by the small lattice mismatch. This is in agreement with our results, as all of the Ge-GaAs IF states lie below the valence-band maximum.

The band-edge discontinuities of a large number of IF's have been extracted from experimental

data, usually $C-V$ and $I-V$ studies, but due to the spread in published values there remain problems in determining the best value for a particular IF. One difficulty is the extraction of doping-level-independent quantities, in this case band-edge discontinuities, from $C-V$ and $I-V$ spectra which are highly dependent on doping level. In the earlier days, when it was desirable to remove some variable(s) from the problem, a simplification was introduced by assuming that the conduction-band discontinuity is equal to the difference in electron affinities. This simplification has often been treated as a rigorous result which, as noted by Kroemer,¹² is not the case. However, Shay *et al.*¹¹ have recently argued that this simple model should be at least approximately satisfied.

There is also no assurance that the band-edge discontinuities are independent (or even nearly so) of the crystallographic IF considered, although this has nearly always been assumed. One available study by Fang and Howard²⁵ indicates a difference of ~ 0.3 eV in band-edge discontinuities between Ge-GaAs [Ga(111)] and [As(111)] IF's, but more work is needed before definite conclusions are warranted.⁴ Finally we note that most IF's have been graded to some, usually unknown, extent; this should tend to decrease the measured values of both ΔE_c and ΔE_v . Recent studies²⁶ of $\text{Al}_x\text{Ga}_{1-x}\text{As}$ -GaAs "abrupt" IF's grown by liquid-phase epitaxy indicates that this junction is usually graded over a width of ~ 100 Å. This level of grading may decrease significantly the measured band-edge discontinuities, since calculations²⁷ for graded IF's indicate that grading over 300 Å completely removes the energy-band barriers. With these caveats in mind we proceed to a comparison of our results for ΔE_c and ΔE_v with experiments and with other theoretical estimates.

Results are not available on single AlAs-GaAs IFs due to the difficulty in preparing the AlAs compound appropriately. As noted in Sec. III, our values for the band-edge discontinuities for AlAs-GaAs are in excellent agreement with extrapolations from the measurements of Dingle *et al.*^{17,23} and Esaki and co-workers.^{16,24} The measurements were taken on $\text{Al}_x\text{Ga}_{1-x}\text{As}$ -GaAs superlattices ($x \sim 0.2$) grown by molecular beam epitaxy, where grading effects can be very small.^{16,17} Both (110) and (100) IFs have been studied by these methods, with no differences having been reported. There is no experimental evidence of IF states or strain in these superlattices. All of these results are consistent with our finding that the change from AlAs to GaAs across the IF occurs with negligible disruption of the bonds.

The first theoretical predictions of band-edge discontinuities were made by Frensley and Kroe-

mer⁹ by assuming that the average interstitial potential is continuous across the IF. For AlAs-GaAs they found $\Delta E_v = 0.26$ eV, in good agreement with our results and experiment. A revised version²⁸ of their model, which gives better agreement with experiment for most IFs they consider, gives the poorer value $\Delta E_v = 0.69$ eV for this IF. Using a tight-binding-like model Harrison¹⁰ has found $\Delta E_v = 0.01$ eV for $\text{Al}_{0.2}\text{Ga}_{0.8}\text{As}$ -GaAs, which is near the experimental value. An experimental value of the electron affinity of AlAs is apparently not available. Shay *et al.*,¹¹ however, argue that a theoretical estimate of this quantity indicates that the "electron affinity rule" is reasonably well satisfied in this system. The result of this paper is the first self-consistent prediction of ΔE_v and ΔE_c for the AlAs-GaAs IF.

As mentioned in Sec. III, experimental values of the band-edge discontinuities in Ge-GaAs are rather widely spread, with values of ΔE_c ranging from²⁹ 0.11 to⁴ 0.40 eV. The majority of published values, however, tend to lie in the lower half of this range. Our result, $\Delta E_c = 0.40$ eV, is not inconsistent with the data but is perhaps ~ 0.2 eV higher than the most probable value. The estimates of Frensley and Kroemer⁹ ($\Delta E_c = 0.03$ eV) and of Shay *et al.*¹¹ ($\Delta E_c = 0.06$ eV) are perhaps somewhat closer to the experimental data, while Harrison's¹⁰ value ($\Delta E_c = 0.35$ eV) is similar to our result. The only previous self-consistent estimate is for the (100) IF, where BAH¹³ found $\Delta E_c \approx 0$ for the ideal IF, and $\Delta E_c \approx -0.1$ eV for their proposed relaxation. Both of the IF's studied by BAH are metallic and it is unclear whether the band-edge discontinuities will be affected by this.

In the literature there appears to be some confusion concerning the origin of the band-edge discontinuities across an IF, or equivalently, the difference $\Delta \bar{V}$ in average potential across the IF. In the calculations described here $\Delta \bar{V}$ is the sum of only three contributions. First, there is a difference in average ion core potential $\Delta \bar{V}_{\text{ion}}$. BAH,¹³ in the study of the (100) IF of Ge-GaAs, restricted their potentials such that $\Delta \bar{V}_{\text{ion}} \equiv 0$. This has not been done in the work described here, as can be seen in Fig. 2. Secondly, there is a difference in average Hartree potential $\Delta \bar{V}_H$, which includes the dipole (3) as well as other (very small) contributions depending on the details of the self-consistent charge density. Finally, there is a difference in average exchange-correlation potential $\Delta \bar{V}_{xc}$ which can be obtained from bulk calculations. Using the Wigner interpolation procedure BAH¹³ have found $\Delta \bar{V}_{xc} = 0.09$ eV for Ge-GaAs. Using the statistical $\rho^{1/3}$ approximation we find differences in \bar{V}_{xc} for Ge, GaAs, and AlAs to be less than 0.01 eV (assuming equal atomic volumes).

B. Possible relaxation at the Ge-GaAs (110) interface

The peculiar bonds across the Ge-GaAs IF, together with a lack of precise agreement with the experiment values of ΔE_c and ΔE_v , suggests relaxation, or possibly reconstruction, at this IF. Since the bonds are "nonideal" in that they do not contain exactly 2 electrons, the resulting weakening of the bonds suggests a simple separation of the planes at the (110) IF. This relaxation is in the direction to bring the band edges into better agreement with experiment, since for infinite separation ΔE_c is equal to the difference in electron affinities (0.06 eV).³⁰

The "nonideal" bonds can be considered in another fashion, with predictions conflicting with a simple separation of the planes at the IF. The Ge-As bond contains 2.11 electrons, but below a well-defined gap, and hence all in bonding states. Thus the Ge-As bond is almost certain to be stronger than the bulk Ge-Ge or Ga-As bonds. There is little doubt that the Ge-Ga bond is weaker than the bulk bonds. These considerations suggest a "tipping" of the Ga-As bonds adjacent to and parallel to the IF, with the Ge-As bond contracting and the Ge-Ga bond distending. This is the more suggestive since it is similar to the apparent relaxation³¹ at the GaAs (110) surface, but its effect on the band edges is difficult to estimate. Research on possible relaxation at this IF is continuing.

C. Interface states and surface states

One approach to the understanding of the origin of IF states is in terms of surface states, and how IF states arise, or evolve from surface states, as two surfaces are "brought together" to form an IF. Since both surface and IF states can be interpreted in a real space picture, e.g., as *s*-like states, dangling bonds, etc., this suggests that an intimate relationship between IF states and surface states may exist. We will discuss these interconnections qualitatively here.

The surface states of the ideal GaAs (110) interface have been well characterized theoretically^{18,32} and will be discussed below. Unfortunately, the ideal Ge (110) surface has not been studied theoretically. However, extrapolating from GaAs, it can be expected that the (110) Ge surface will have dangling bonds states in or near the gap. Parallel or back bonds, as well as *s*-like states, may appear at lower energies but the following discussion will not depend on these details.

We will use the results of Chelikowsky and Cohen¹⁸ for the surface states of (110) GaAs, since the self-consistent pseudopotential method was used for their calculations. In addition the Ga and

As ionic pseudopotentials are the same as those used in our IF calculations. The surface states and energies (on the energy scale of our Ge-GaAs IF) are listed in Table II, together with our results for the Ge-GaAs (110) IF. The arrows in Table II denote the relationships of surface states to IF states.

We begin in the low-energy region. The As *s*-like IF state lies 2.25 eV below its surface counterpart, while the Ga *s*-like IF state is at approximately the same energy as the corresponding surface state. The behavior of the As *s*-like state is clear: the surface pushes it above the bulk As *s*-like states, while the Ge slab (or probably just the Ge nearest neighbor) pulls it below. The Ga *s* state at the "edge" (surface or IF), however, sees both the surface and the neighboring Ge atom as a positive perturbation compared to a Ga *s* state in the bulk, surrounded by As atoms. These two positive perturbations have similar results, giving rise to a localized state near the bottom of the stomach gap (Fig. 5).

From Fig. 6 we see that the Ge-As bonding state B_1 at the IF can be considered as derived from dangling bonds and back bonds of the As atom on the GaAs surface and the Ge atom at the Ge surface. The potential in the dangling bond region will be greatly reduced in bringing the surfaces together. This is reflected in the 3.5 eV difference in energies of the As (and presumably Ge) dangling bond and the Ge-As bonding state. The development of the Ge-Ga bonding state B_2 can be viewed similarly, with the difference between Ga (and Ge) dangling bonds and the Ge-Ga bonding state being ~2 eV.

The parallel bonding IF states P_1 and P_2 can qualitatively be regarded as arising from parallel bond surface states in Ge and in GaAs. However, without specific information on the Ge surface states this identification cannot be carried any further.

We can tentatively conclude that, in IFs in semiconductors with negligible lattice mismatch, the study of the ideal surfaces can be useful in predicting the existence and character of IF states.

D. Superlattice states in AlAs-GaAs

Recently, molecular beam epitaxy methods^{16,17} have been used to construct AlAs-GaAs and $\text{Al}_x\text{Ga}_{1-x}\text{As}$ -GaAs (as well as other) superlattices. Superlattices can be grown with either (110) or (100) IF's, with no differences between these two alternatives having been reported. Characterizations of the superlattices indicate an alternating epitaxy of high quality. Experiments on superlattices include *I-V* and photocurrent measurements

by Esaki and coworkers,^{16,24} and optical absorption by Dingle and collaborators.^{17,23} The data have been interpreted in terms of states quantized in the z direction (the superlattice direction). The presumption is that the valence- and conduction-band discontinuities form effective potential wells which contain a few quantized energy levels and confine carriers in these levels to the material with smaller band gap. Superlattices have typically involved ~ 25 – 50 layers of each material and interpretation of data using this approach has been very successful.

In our calculations involving 9 layers of each material superlattice states are found to exist; however, for this "small" unit cell each state can overlap appreciably with the corresponding state in the next unit cell ("potential well") so a direct comparison to single-well states may not be appropriate. We concentrate on the AlAs-GaAs system since it has been of most experiment interest. We describe in particular the states near the valence-band maximum at Γ , since our results are most realistic in this region.

At the Γ point we find the two uppermost occupied states (just below the fundamental gap) are superlattice states, in that their charge density is confined almost entirely to GaAs. We refer to these as superlattice hole (SLH) states. The third state below the gap has equal charge in AlAs and GaAs and is clearly below the valence-band maximum of each material, and is therefore not what is usually referred to as a superlattice state. The SLH states are split in energy by 0.05 eV, with the "higher" energy hole state ψ_2 (near the "top" of the inverted potential well for holes) being just bound. (It is difficult to give precise energies relative to the bottom of the potential well since for our 9-layer-9-layer structure the bulk band edges are not precisely defined.) In either Ge or GaAs in the bulk the two top valence states at Γ are degenerate. This splitting is the direct result of the lowering of symmetry in the IF and has been observed experimentally in both superlattice²³ and monolayer³³ structures. It is natural to try to interpret these states as the light- and heavy-hole states in the potential wells. However, this description appears not to apply to these states, for the following two reasons.

The usual assumption is that the superlattice light hole state(s) ψ_{lh} is (are) given *roughly* by deep square well (or standing wave) form

$$\psi_{\text{lh}}(x, y, z) \sim \psi_{\text{lh}}^{(\text{bulk})}(x, y, z) \times \begin{cases} \cos(n\pi z/2c), & n \text{ odd,} \\ \sin(n\pi z/2c), & n \text{ even,} \end{cases} \quad (4)$$

where $\psi_{\text{lh}}^{(\text{bulk})}$ is the light-hole state in the bulk, the

well region is $|z| < c$, and the heavy-hole state is given similarly (the energies, however, are calculated for the appropriate finite square well). The charge densities of both states for $n=1$ would then be bulklike except near the edges of the potential well. We find however that the lower-energy SLH state ψ_1 has its charge density confined to GaAs bonds *parallel* to the IF, with no charge in the chains of bonds perpendicular to the IF. The charge density of ψ_2 conversely lies primarily in the chains of bonds perpendicular to the IF. The formation of these states is apparently the result of a quantized state in one well interacting with states in neighboring wells. Such states, which apparently have not been predicted previously, should be detectable by optical studies using polarized radiation. The appearance of these states indicate that the specific superlattice geometry we have used is intermediate between the quantized superlattices states studied experimentally and the repeated monolayer structures, which are essentially new compounds, studied theoretically by Caruthers and Lin-Chung.¹⁴

Secondly, we have calculated the effective masses for the states ψ_1 and ψ_2 , using the usual expression from $\vec{k} \cdot \vec{p}$ perturbation theory. For ψ_1 we find $m_x^* = 0.10$, $m_y^* = 0.42$, and $m_z^* = -0.93$, in units of the free-electron mass. The x and y directions are shown in Fig. 1. For ψ_2 , we find $m_x^* = 0.43$, $m_y^* = 0.17$, and $m_z^* = 0.73$. The bulk (isotropic) effective hole masses in GaAs are ~ 0.6 and 0.07 . Referring to the transverse effective masses m_x^* and m_y^* , it is evident that neither state is clearly identifiable as a light- or heavy-hole state.

Even if our calculations were exact these details would hold only for 9-layer-AlAs-9-layer-GaAs superlattices with (110) IFs. However, similar effects can be expected to occur in other few-layered superlattices. Here we want primarily to emphasize that the character and transverse as well as parallel effective masses of superlattice bands can be sensitive to coupling between potential wells. In experiments on few-layered superlattices coupling between well states has been observed,²³ but effective masses have not been extracted from the data.

V. CONCLUSIONS

Our results for the ideal AlAs-GaAs (110) IF agree well with experimental results where comparison is available. The disruption of the bulk electronic structure at the IF, as evidenced by both the bond charge density and local density of states, is very minor for this system. In particular there is no indication that reconstruction or even appreciable relaxation will occur this IF.

The ideal Ge-GaAs (110) IF is found to possess a sizable density of IF states, which may be measurable in very careful photoemission studies of a few monolayers of Ge on GaAs (110). There are no IF states in the fundamental gap, in agreement with experimental results on heterojunctions. The Ge-Ga and Ge-As bonds across the IF are found to be considerably different from either Ge-Ge or Ga-As bonds in the bulk, which suggests relaxation at this IF.

We have proposed two possible relaxations. The first is a simple separation of the atomic planes at the IF which, in addition to being the simplest possible relaxation, has the virtue that it will force the band-edge discontinuities into agreement with experiment for some value of the separation.

The second proposed relaxation is that the GaAs plane at the IF will tip so as to shorten the Ge-As bond and lengthen the Ge-Ga bond. This relaxation is suggested by the nature of the bonds across the ideal IF, and is similar to the relaxation which has been found at the GaAs (110) surface.

ACKNOWLEDGMENTS

We would like to thank Dr. J. C. Phillips, Dr. M. Schlüter, Dr. J. A. Appelbaum, and Dr. D. R. Hamann for useful discussions. We also thank Dr. G. Kerker, K. M. Ho, and J. Ihm for helpful comments during the course of this work. Part of this work was supported by NSF Grant No. DMR76-20647 and part under the auspices of the U.S. ERDA.

*Supported by IBM.

†Supported by the NSF. Present address: IBM Watson Research Center, Yorktown Heights, N.Y. 10598.

¹V. Heine, Proc. Phys. Soc. **81**, 300 (1963).

²See, for example, B. D. Kandilarov, V. Detcheva, and P. C. Petrova, Phys. Status Solidi **70**, 775 (1975), and references therein.

³For a recent review see F. Jona and P. M. Marcus, Comments Solid State Phys. **8**, 1 (1977), and references therein.

⁴A. G. Milnes and D. L. Feucht, *Heterojunctions and Metal-Semiconductor Junctions* (Academic, New York, 1972).

⁵B. L. Sharma and R. K. Purohit, *Semiconductor Heterojunctions* (Pergamon, New York, 1974).

⁶A. J. Bennett and C. B. Duke, Phys. Rev. **160**, 541 (1967); J. Heinrichs and N. Kumar, Phys. Rev. B **12**, 802 (1975); R. M. Nieminen, J. Phys. F **7**, 375 (1977).

⁷S. G. Louie and M. L. Cohen, Phys. Rev. B **13**, 2461 (1976); S. G. Louis, J. R. Chelikowsky, and M. L. Cohen, J. Vac. Sci. Technol. **13**, 790 (1976).

⁸J. Bardeen, Phys. Rev. **71**, 717 (1947); V. Heine, Phys. Rev. **138**, A1689 (1965); J. C. Inkson, J. Phys. C **5**, 2599 (1972).

⁹W. R. Frensley and H. Kroemer, J. Vac. Sci. Technol. **13**, 810 (1976).

¹⁰W. A. Harrison, J. Vac. Sci. Technol. **14**, 1016 (1977).

¹¹J. L. Shay, S. Wagner, and J. C. Phillips, Appl. Phys. Lett. **28**, 31 (1976).

¹²H. Kroemer, Crit. Rev. Solid State Sci. **5**, 555 (1975).

¹³G. A. Baraff, J. A. Appelbaum, and D. R. Hamann, Phys. Rev. Lett. **38**, 237 (1977); J. Vac. Sci. Technol. **14**, 999 (1977).

¹⁴E. Caruthers and P. J. Lin-Chung, Phys. Rev. Lett. **38**, 1543 (1977).

¹⁵W. E. Pickett, S. G. Louie, and M. L. Cohen, Phys. Rev. Lett. **39**, 109 (1977).

¹⁶L. Esaki and L. L. Chang, Crit. Rev. Solid State Sci. **6**, 195 (1976).

¹⁷R. Dingle, Crit. Rev. Solid State Sci. **5**, 585 (1975).

¹⁸J. R. Chelikowsky and M. L. Cohen, Phys. Rev. B **13**, 826 (1976).

¹⁹A. Baldereschi, Phys. Rev. B **7**, 5212 (1973); D. J. Chadi and M. L. Cohen, *ibid.* **8**, 5847 (1973).

²⁰J. R. Chelikowsky and M. L. Cohen, Phys. Rev. B **14**, 556 (1976).

²¹The charge density on the AlAs side of the IF was compared with self-consistent pseudopotential calculations of the bulk AlAs charge density [W. E. Pickett, S. G. Louis, and M. L. Cohen (unpublished)].

²²For AlAs see C. A. Mead and W. G. Spitzer, Phys. Rev. Lett. **11**, 358 (1963).

²³R. Dingle, A. C. Gossard, and W. Wiegmann, Phys. Rev. Lett. **34**, 1327 (1975); R. Dingle, W. Wiegmann, and C. H. Henry, *ibid.* **33**, 827 (1974).

²⁴R. Tsu, L. L. Chang, G. A. Sai-Halasz, and L. Esaki, Phys. Rev. Lett. **34**, 1509 (1975).

²⁵F. F. Fang and W. E. Howard, J. Appl. Phys. **35**, 612 (1964).

²⁶C. M. Garner, V. D. Shen, J. S. Kim, G. L. Pearson, W. E. Spicer, J. S. Harris, Jr., and D. D. Edwall, J. Appl. Phys. **48**, 3147 (1977); C. M. Garner, Y. D. Shen, J. S. Kim, G. L. Pearson, W. E. Spicer, J. S. Harris, D. D. Edall, and R. Sahai, J. Vac. Sci. Technol. **14**, 985 (1977).

²⁷W. G. Oldham and A. G. Milnes, Solid State Electron. **6**, 121 (1963); D. T. Cheung, S. Y. Chiang, and G. L. Pearson, *ibid.* **18**, 263 (1975).

²⁸W. R. Frensley and H. Kroemer (unpublished).

²⁹J. P. Donnelly and A. G. Milnes, IEEE Trans. Electron Dev. **ED-14**, 63 (1967).

³⁰G. W. Gobeli and F. G. Allen, Phys. Rev. **137**, A245 (1965).

³¹J. E. Rowe, S. B. Christman, and G. Margaritondo, Phys. Rev. Lett. **35**, 1471 (1975); J. R. Chelikowsky, S. G. Louie, and M. L. Cohen, Phys. Rev. B **14**, 4724 (1976).

³²J. D. Joannopoulos and M. L. Cohen, Phys. Rev. B **10**, 5075 (1974); C. Calandra and G. Santoro, J. Phys. C **8**, L86 (1975); N. Garcia, Solid State Comm. **17**, 397 (1975).

³³J. P. van der Ziel and A. C. Gossard, J. Appl. Phys. **48**, 3018 (1977).